Available online at www.sciencedirect.com
ScienceDirect
Carbohydrate Polymers 67 (2007) 417–426
Carbohydrate Polymers
www.elsevier.com/locate/carbpol

Surface biofunctionalization of PLA nanoparticles through amphiphilic polysaccharide coating and ligand coupling: Evaluation of biofunctionalization and drug releasing behavior

Ming-qi Gu [a,1], Xu-bo Yuan [a,*], Chun-sheng Kang [a,b,1], Yun-hui Zhao [a], Neng-jiang Tian [c], Pei-yu Pu [b], Jing Sheng [a]

[a] School of Materials Science and Engineering, Tianjin University, Tianjin 300072, China
[b] Department of Neurosurgery, Tianjin Medical University General Hospital, Tianjin 300052, China
[c] Immunology Laboratory of Urinarysurgery Institute, Tianjin Medical University, Tianjin 300052, China

Received 13 March 2006; received in revised form 25 May 2006; accepted 8 June 2006
Available online 8 August 2006

Abstract

The purpose of present study was to conceive small-sized nanoparticles which can be easily functionalized with ligands and meanwhile minimized drug leakage. For this purpose, cholesterol-modified dextran dialdehyde was synthesized and used to prepare indomethacin loaded PLA nanoparticles containing aldehyde groups on surface. Transferrin (TF) was coupled to their surface by taking advantage of the Schiff's base reaction and the effect of ligand coupling on drug leakage was evaluated. The results show that the coupling process reached equilibrium within 5 min and less than 20% drug was leaked after $NaBH_4$ reduction. TF coupled nanoparticles was fluorescence labeled with FITC, and cell uptake experiment was performed in vitro. The result demonstrated the bioactivity of TF after binding on nanoparticles and the ability of the nanoparticles targeting to tumor cell mediated by ligand–receptor interaction.

Keywords: Amphiphilic polysaccharide; Nanoparticles; Transferrin; Biofunctionalization; Drug leakage

1. Introduction

Poly(lactic acid) (PLA) and its copolymer nanoparticles have shown great potential as carrier systems for an increasing number of active molecules, largely due to the excellent biocompatibility and the controlled biodegradability properties. However, the main drawback of these carriers is their non-specific interaction with cells and proteins, leading to drug accumulation in non-target tissues (Lemarchand, Gref, & Couvreur, 2004; Bazile et al., 1995; Mora & Baraldi, 2002). To overcome this problem, many studies have been devoted to surface functionalization of PLA nanoparticles, namely, active target delivery system (ATDS).

The active target delivery of drug need the carriers (i) minimize interaction with plasma and (ii) target cell surface receptors (Nobs, Buchegger, Gurny, & Allemann, 2004). Poly(ethylene glycol) (PEG) coating could delayed the phagocytosis of nanoparticles, avoiding the mononuclear phagocyte system (MPS) sequestration. But PEG-coated nanoparticles cannot provide specific targeting, and their final destination was always the MPS (Mora & Baraldi, 2002). In order to achieve an active targeting, specific ligands must be attached to nanoparticles surface to enable molecular recognition. However, chemical coupling of such ligands is usually very difficult because of the absence of reactive groups at the surface of pegylated carriers (Stella et al., 2000).

Polysaccharides constitute an important class of physiological materials. They display well-documented biocompatibilities and biodegradabilities, which are the basic

* Corresponding author. Tel.: +86 22 27402702; fax: +86 22 27404724.
E-mail address: xbyuan@tju.edu.cn (X. Yuan).
[1] Authors contribute equally to the present work.

0144-8617/$ - see front matter © 2006 Elsevier Ltd. All rights reserved.
doi:10.1016/j.carbpol.2006.06.019

characteristics for polymers used as biomaterials (Dumitriu, 2001). The surface modification by polysaccharide increased the *in vivo* half-life of nanoparticles in the same way as PEG did (Woodle & Lasic, 1992; Allen, 1994; Rouzes, Gref, Leonard, & Dellacherie, 2000; Choi, Kim, & Kim, 2003), and the enrichment in reactive groups make them are more easily to couple ligands.

Although some polysaccharide decorated PLA nanoparticles have been prepared successfully, the ligand conjugation is still a challenge work, because inappropriate conjugation method will lead to, on the one hand, the loss of bioactivity of ligand (Nobs et al., 2004), and on the other hand, the leakage of the pre-entrapped drug (Lundberg, Griffiths, & Hansen, 2000), resulting in the fail in the clinic application. To our knowledge, however, only a few papers have addressed this issue so far. The present paper focus on the biofunctionalization of polysaccharide decorated PLA nanoparticles and its effect on the drug-loading and release behavior. For these purposes, cholesterol hydrophobic modified dextran dialdehyde (Chol-Dex-CHO) was synthesized. Indomethacin (IMC) loaded PLA nanoparticles coated with Chol-Dex-CHO were prepared using diafiltration method, and transferrin (TF), chosen as model ligands, was coupled to nanoparticles *via* Schiff's base reaction. The optimum conditions for the surface functionalization and drug-loading were investigated, and the tumor cell targeting was evaluated by glioma cell uptake experiment in vitro.

2. Experimental

2.1. Materials

PLA ($M_w = 30$ kDa) was purchased from Sigma. Dextran ($M_n = 40$ kDa) was from Amersham Biosciences (Uppsala, Sweden). Cholesterol was obtained from Tianjin Chemical Reagent Co., China, and recrystallized in ethanol before use. Indomethacin was purchased from Tianjin Pharmaceutical Group Corporation, China. Transferrin and fluorescein isothiocyanate (FITC) was obtained from Sigma. The water used in these studies was double distilled and all other reagents and organic solvents used were reagent grade or better. Fuchsin solution was prepared as follows.

0.5 g powdered basic fuchsin was dissolved in about 100 mL hot water in a 200 mL flask, and 20 mL sodium sulphite aqueous solution (0.15 g/mL) was added. After 10 min 6 mL hydrochloric acid was added and the solution turned colorless, the flask was capped tightly and stored at room temperature in the dark for 72 h, shaking occasionally to dissolve pink precipitate.

2.2. Synthesis and characterization of cholesterol hydrophobically modified dialdehyde dextran derivatives

Cholesterol-modified dextran derivates containing aldehyde groups (Chol-Dex-CHO) was synthesized by esterifying of hydroxyl groups of dextran dialdehyde with cholesterol 3-hemisuccinyl chloride. The detail processes were described as follows.

2.2.1. Synthesis of cholesterol 3-hemisuccinyl chloride

One gram of succinic anhydride was added per gram of cholesterol and dissolved in 30 mL of pyridine. The mixture was stirred for 3 h at 70 °C. The crude product was dissolved in a minimum amount of H_2O/ethanol (1:10,v/v), and cholesterol 3-hemisuccinate was crystallized from H_2O/methanol (1:10,v/v), then recrystallized from ethanol (Kuhn, Schrader, Smith, & O'Malley, 1975).

One gram of cholesterol 3-hemisuccinate was dissolved in 30 mL anhydrous chloroform, and an excess of $SOCl_2$ (10-fold) in 10 mL anhydrous chloroform was added dropwise under nitrogen protecting. The reaction mixture was stirred vigorously at 60 °C for 4 h, then the solution was evaporated under vacuum to remove solvent and the remained $SOCl_2$, the residue was kept in anhydrous chloroform airproofly.

2.2.2. Synthesis of Chol-Dex-CHO

Oxidation of dextran was performed in 30 mL distilled water (Schacht, Bogdanov, Van Der Bulcke, & De Rooze, 1997; Svetlana, Ludmila, Alexander, & Elena, 1996), which contained dextran (2 g) and $NaIO_4$ (IO_4^-/glucopyranosidic units = 1/20). The mixture was stirred vigorously at room temperature for 8 h followed by dialyzed against deionized water for 72 h. Then the dextran dialdehyde (Dex-CHO) was obtained by freeze-drying. The content of aldehyde groups was estimated to be 0.235 mmol/g Dex-CHO by Schales' method with the calibration curve of glutaraldehyde (Imoto & Yanagishita, 1971).

For the synthesis of Chol-Dex-CHO, 500 mg Dex-CHO was dissolved in 40 mL anhydrous DMSO, and 0.3 mL triethylamine was added. After the mixture was heated up to 80 °C, 0.3 mmol Chol-succ-COCl in 4.4 mL $CHCl_3$ was added dropwise. The reaction was performed for 8 h under nitrogen protecting. Then Chol-Dex-CHO was obtained by dialysis of product against deionized water and freeze-drying.

The structure of Chol-Dex-CHO was confirmed by FT-IR (Bio-Rad FTS 135, Perkin-Elmer Co., US) and ^1H NMR (DMSO-d_6, Varian UMTY plus400 NMR spectrometer).

2.2.3. Surface tension measurement

The surface tensions were measured with a Dataphysics DCTA-21 dynamic contact-angle analyzer (Bad Vilbel, Germany) using the Wilhelmy plate method. The instrument was calibrated against distilled water, and before each measurement the platinum plate was cleaned by heating to a red/orange color with a alcohol burner. Measurements were taken at 25 ± 0.1 °C. The 20-mL Chol-Dex-CHO solutions were prepared at concentrations ranging from 1×10^{-5} to 1 mg/mL using distilled water. All sample solutions were aged before use.

2.2.4. Fluorescence spectroscopy

The fluorescence spectroscopy was measured with a Spectrofluorophotometer (F4500 model, HITACHI, Jap), using pyrene as a hydrophobic probe. Sample suspensions were prepared by adding a known amount of pyrene in acetone to a series of 20 mL vials, and then removing the acetone by evaporation to a final pyrene concentration of 6.0×10^{-7} M. Various concentrations (10 mL) of CS-CHOL conjugate suspension were then added to each vial and heated for 3 h at 65 °C to equilibrate the pyrene and the nanoparticles, and then remained undisturbed to cool overnight at room temperature. For measurement of the intensity ratio of the first and the third highest energy bands in the emission spectra of pyrene, the slit openings for excitation and emission were both set at 2 nm. The excitation wavelength (λ_{ex}) was 336 nm.

2.3. Preparation of PLA/Chol-Dex-CHO nanoparticles

The nanoparticles were prepared by a co-dialysis method. In detail, 8 mg PLA and 40 mg Chol-Dex-CHO were co-dissolved in 20 mL dimethyl sulphoxide (DMSO) with magnetic stirring. The resultant solution was dialyzed against deionized water under ice-bath for 72 h. Then the resulting suspension was centrifuged at 16,000*g* for 10 min, followed by washing three times with normal saline under sonication. PLA/Chol-Dex-CHO nanoparticles were obtained by freeze-drying finally.

When drug loaded nanoparticles were prepared, 2 mg IMC was added into PLA and Chol-Dex-CHO in DMSO solution. The IMC loaded nanoparticles were prepared in the same procedure as described above.

2.4. Surface functionalization of the nanoparticles with TF

2.4.1. Content of aldehyde groups on PLA/Chol-Dex-CHO nanoparticles

Five milliliters of fuchsin solution was added to 20 mL functionalized nanoparticle suspension (0.05 mg/mL). The color was allowed to develop for 30 min, then the absorbance value of the solution at 550 nm was determined using a HP8453 UV–visible spectrophotometer. To make a reference, nanoparticles composed of PLA and cholesterol-modified dextran were prepared, and the concentration of reference was also adjusted to 0.05 mg/mL. Fuchsin solution was added following the same procedure. The content of aldehyde groups on the nanoparticles was calculated with the calibration curve of glutaraldehyde.

2.4.2. Saturation for the TF coupling on nanoparticles

The maximum amount (saturation) for the ligand coupling on the PLA/Chol-Dex-CHO nanoparticles was investigated by UV–visible spectrophotometer measurement. Briefly, different amounts of TF were added to the PLA/Chol-Dex-CHO nanoparticles borate buffer solution (pH 9.18, concentration of nanoparticles = 1 mg/mL). After being incubated overnight at 25 °C, the suspensions were submitted to centrifugation. The supernatants were collected and the TF remaining in the solution was measured by ultraviolet spectrophotometry (measured at 260 nm). The saturation for the ligand coupling was determined by plotting the curve of absorbance versus weight ratio of TF to nanoparticles, and the saturation ratio was defined as the ratio that above which no more of TF could coupled on the nanoparticles.

2.4.3. Evaluation of coupling reaction

7.2 mg TF was dissolved in 10 mL borate buffer solution (pH 9.18), the solution obtained was added to 60 mL IMC-loaded PLA/Chol-Dex-CHO nanoparticles borate buffer solution (concentration of nanoparticles = 2 mg/mL). The mixture was incubated at 25 °C in a water bath. At defined time intervals, 5 mL incubated solution was taken out and the surface-functionalized nanoparticles were separated by centrifugation (MR1822, JOUAN Co., France) at 16,000*g* for 10 min, followed by washing with double distilled water under sonication. This procedure was repeated three times, and the supernatants were collected. The TF remaining after incubation reaction was determined by ultraviolet spectrophotometry (measured at 260 nm). The surface-functionalized nanoparticles obtained were separated into three parts, two parts for the evaluation of drug leakage and drug release behavior after surface-functionalization process, respectively. The additional part was used to determinate the residual amount of aldehyde groups after incubation reaction by the same procedure mentioned in Section 2.4.1.

The drug leakage was evaluated as follows: surface-functionalized nanoparticles were freeze-dried, and then dissolved in 0.5 mL methylene chloride followed by adding 5 mL ethanol to precipitate the polymer. The suspension was centrifuged at 16,000*g* for 20 min, the supernatants were collected and the amount of IMC was determined spectrophotometrically at 340 nm. The drug leakage rate was defined by the following function:

$$\text{Drug leakage } (\%) = \frac{M_{PE} - M_{AF}}{M_{PE}} \times 100$$

where M_{PE} is the mass of drug pro-entrapped in the nanoparticles, while M_{AF} is the mass of drug loading of nanoparticles after biofunctionalization.

The drug release of the nanoparticles in vitro was performed as follows: freeze-dried nanoparticles were placed in dialysis bags, which were incubated in vials containing PBS (pH 7.4). The vials were placed in a thermostatic vibrator at 37 °C. The solution was replaced at specified time intervals during one week incubation period. The concentration of IMC in the recovered solution was determined by spectrophotometry at 340 nm.

2.5. Nanoparticles characterization

2.5.1. Size and morphology

To evaluate the effect of biofunctionalization on nanoparticle size, nanoparticle size analyses were carried out

on a particle size analyzer (PSA, Brookhaven Instruments Corp. 90 Plus, USA). The nanoparticle was dispersed in physiological saline and sonicated for 2 min at 40 W, then their effective diameter was recorded at 90° scattering angle under 25 °C without filtering.

The morphology of the PLA/Chol-Dex-CHO nanoparticles was observed using a transmission electron microscope (TEM) (JEM-2000 FX II, Jeol, Japan). A drop of the nanoparticle suspension was placed on a copper grid coated with carbon film and dried at 25 °C. Observation was performed at 80 kV.

2.5.2. Surface analysis

XPS spectra were obtained using PHI-1600 electron spectrometer (Perkin-Elmer Co., US), in which Al Kα radiation (1486.6 eV) at 50 W anode power and a pass energy at 50 eV were employed. Survey scans were collected from 0 to 1200 eV with the pass energy of 50 eV for each sample followed by the C_{1s}, N_{1s}, and O_{1s} regions. Data processing was performed using ECLIPSE program applying Shirley-type background subtraction. Curve-fitting was performed using the nonlinear least-squares algorithm and assuming a mixed Gaussian/Lorentzian peak shape of variable proportion. This peak-fitting was repeated until an acceptable fit was obtained.

2.5.3. Zeta potential

Zeta potential of PLA, Chol-Dex-CHO, PLA/Chol-Dex-CHO and TF-bound PLA/Chol-Dex-CHO particles were measured using zeta analyzer (Powereach®, Zhongchen Digital Technology Instrument LTD., Shanghai, China). PLA and Chol-Dex-CHO particles were prepared by simple dialysis of their DMSO solution against water, respectively.

2.6. Fluorescent labeling of nanoparticles and glioma cell uptake in vitro

2.5 mg of TF-bound nanoparticles was dispersed in milliliter isotonic HEPES/NaOH buffer (pH 7.4) and incubated with a 30-fold molar excess of FITC for 10 h. The resulting solution was dialyzed (the membrane cut-off $M_w = 7000$ Da) exhaustively against water until complete removal of free fluorescein. The resulting nanoparticles were lyophilized and stored at 4 °C.

The U251 human glioma cell was maintained in Dulbecco's modified Eagle's medium (DMEM) supplemented with 10% fetal calf serum (FCS) at 37 °C with 5% CO_2 and 95% air. Cells (1×10^5) were plated in 60 mm cell culture dishes to grow overnight until they were 50–80% confluent. Then the cells were trypsinised with 0.125% (w/v) trypsin/EDTA (pH 8.0) and plated into each well of a 12 well plates to grow overnight. The FITC-labeled nanoparticles were filtered and added into each well. At defined time intervals, the growth medium was removed from each well and cell monolayers were rinsed three times with cold PBS. The internalization of TF-PLA nanoparticles by glioma cells was observed and recorded by phase-contrast fluorescent microscopy, Olympus, Japan.

To evaluate the target of TF functionalized nanoparticles to tumor cells, Chol-Dex derivates containing hydrazide groups (Chol-Dex-NH_2) was synthesized by reacting Chol-Dex-CHO with adipic dihydrazide followed by reducing with $NaBH_4$. Chol-Dex-NH_2 coated PLA nanoparticles were prepared in the same way as mentioned in Section 2.3. The obtained nanoparticles were labeled with FITC and used as control in cell experiment.

3. Results and discussion

3.1. Synthesis of Chol-Dex-CHO

The conjugation of Dex with Chol-succ was confirmed by the FTIR and ^{1}H NMR spectra. Fig. 1 shows the FTIR spectra of Dex-CHO (b) and Chol-Dex-CHO conjugate (a). The characteristic absorption band of Dex-CHO appeared at 1637 cm^{-1} was assigned to the enol groups, which was formed by aldo-enol transition at neutral pH environment (Svetlana et al., 1996). For the Chol-Dex-CHO conjugation, as compared with Dex-CHO, a new absorption band at 1732 cm^{-1} was observed. This absorption ascribed to the carbonyl groups of ester bonds by which cholesterol was conjugated to the backbone chains of Dex-CHO. These results are evidence of the conjugation of Chol onto the dextran dialdehyde.

The incorporation of Chol to Dex-CHO was also confirmed by ^{1}H NMR spectroscopy. As shown in Fig. 2, the peaks at 4.90 and 4.88 ppm correspond to anomeric protons of the dextran skeleton. Furthermore, peaks at 4.6 and 4.5 ppm correspond to methylene protons of the (α) 1–6 glycosidic linkage, and the peaks at 3.7, 3.4, and 3.2 ppm correspond to the hydroxyl protons (Svetlana

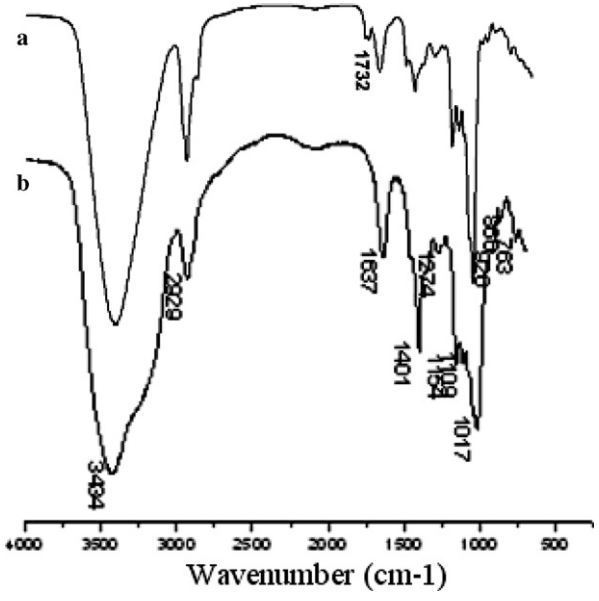

Fig. 1. FTIR spectra of Chol-Dex-CHO (a) and Dex-CHO (b).

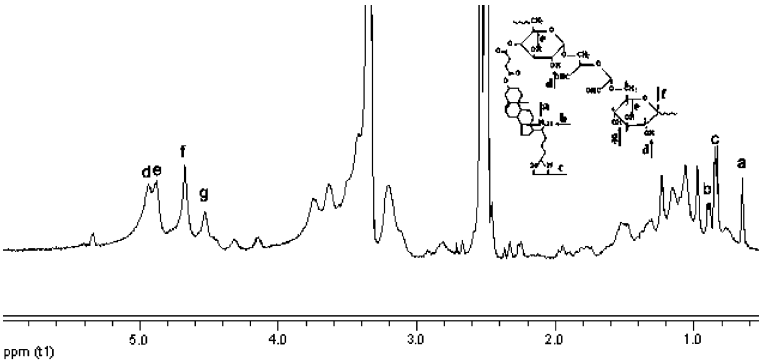

Fig. 2. ^{1}H NMR spectrum of Chol-Dex-CHO conjugates.

et al., 1996; Stenekes, Talsma, & Hennink, 2001). The signals of Chol at 0.59, 0.81, 0.84, and 0.94 ppm were used to assign the protons of CH_3 groups at positions 18, 19, and 21 of the steroid skeleton of Chol (Zipser, Bradford, & Hollingsworth, 1998). The degree of substitution (DS), estimated by the ratio of the integrated area of CH_3 protons at position 18 of the substituent observed in 0.59 ppm over the integrated area of anomeric protons of the dextran skeleton observed at 4.90 and 4.83 ppm, was 8%.

3.2. Amphiphilic characteristic of Chol-Dex-CHO

The surface activity of Chol-Dex-CHO was determined by Wilhelmy surface tension measurement. As shown in Fig. 3, the variation of surface tension with concentration of Chol-Dex-CHO (on log scale) showed a typical surface activity characteristic possessed by many amphiphilic macromolecules (Maiti, Jayachandran, & Chatterji, 2001; Rouzes, Durand, Leonard, & Dellacherie, 2002; Nichifor, Lopes, Carpov, & Melo, 1999).

The amphiphilic characteristic of Chol-Dex-CHO was also confirmed by fluorescence spectrum technology in the presence of pyrene as a fluorescence probe (Vieira, Moscardini, & Tiera, 2003; Alami, Almgren, Brown, & Francois, 1996). Generally, amphiphilic polysaccharide self-aggregate in water and hydrophobic microdomains are usually formed by the association of hydrophobic groups. The pyrene preferably lies close to (or inside) these microdomains and emits fluorescence intensively, and the total emission intensity increases with the concentration of polymeric amphiphiles. Especially the intensity of the third highest vibrational band at 383 nm (I_3) starts to increase drastically at a certain polymer concentration. This concentration is defined as a critical aggregation concentration (CAC), which indicates the threshold concentration of self-aggregation of polymeric amphiphiles (Magmy, Iliopoulos, Zana, & Audebert, 1994; Lee, Jo, Kwon, Kim, & Jeong, 1998).

Fig. 4 shows the fluorescence emission spectra of pyrene incorporated into self-aggregates of Chol-Dex-CHO in water at 25 °C. The fluorescence intensity increased with increasing concentrations of polymer, indicating the aggregation of Chol-Dex-CHO through association of hydrophobic cholesterol component. The critical aggregate concentration (CAC) was determined by measuring the intensity ratio (I_1/I_3) of the first (372 nm) and the third (383 nm) highest energy bands in the emission spectra of pyrene (Fig. 5). The I_1/I_3 values are nearly constant at

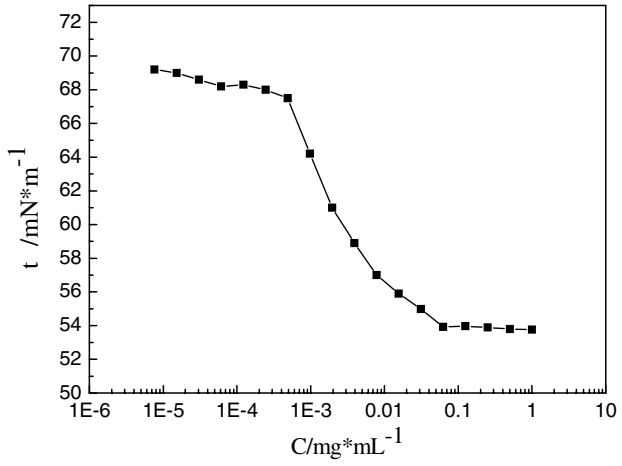

Fig. 3. Variation of surface tension at air/water interface with the Chol-Dex-CHO concentration.

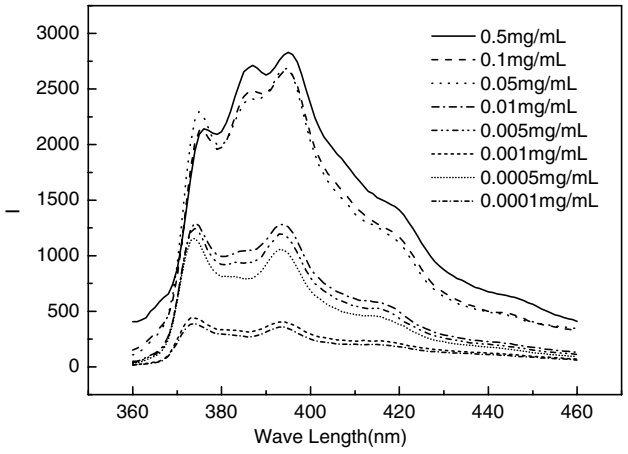

Fig. 4. Fluorescence emission spectra of pyrene (6×10^{-7} M) as a function of Chol-Dex-CHO concentration.

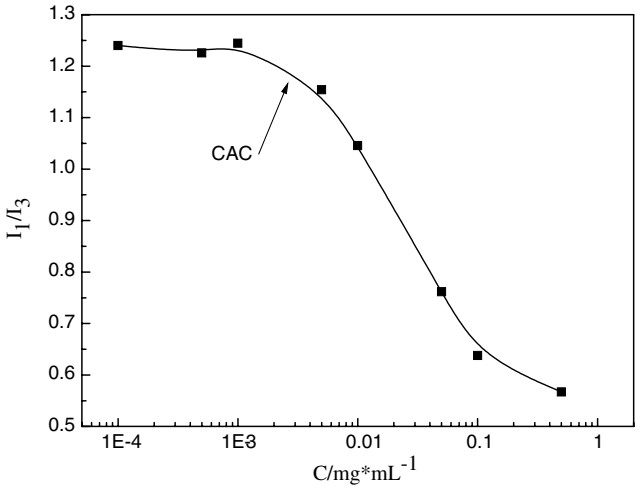

Fig. 5. Plot of intensity ratio (I_1/I_3) of pyrene excitation spectra versus log C of Chol-Dex-CHO.

low concentrations of polymeric amphiphiles, then decrease linearly and reached constant again with the addition of polymeric amphiphiles. The CAC was determined by the first and second inflexion in I_1/I_3—log C curves. Its value was 0.002 mg/mL.

3.3. Characterization of the Chol-Dex-CHO decorated PLA nanoparticles

Chol-Dex-CHO surface-decorated PLA nanoparticles were prepared by a co-dialysis method. The influence of the concentration of Chol-Dex-CHO and its weight ratio to PLA on the formation of nanoparticles was investigated. The results indicated that no matter what the concentration of Chol-Dex-CHO is, the nanoparticles with sphere-like appearance were obtained only when the weight ratio of Chol-Dex-CHO to PLA larger than about 5:1.

The typical TEM image of PLA/Chol-Dex-CHO nanoparticles was shown in Fig. 6. The shapes of nanoparticles obtained were mostly spherical, and a core-shell structure was obviously observed. The size of the hydrated state was measured by laser light scattering without any filtration treatment. As shown in Fig. 7a, a bimodel size distribution was found in the histograms of the size distribution. The diameter of most nanoparticles is in the range of 100–150 nm, while a few of them have a size from 280 to 390 nm.

To verify the presence of Chol-Dex-CHO coating, XPS and zeta potential measurement were carried out. The high-resolution XPS spectra for PLA, Chol-Dex-CHO and PLA/Chol-Dex-CHO nanoparticles are given in Fig. 8. The C_{1s} core level spectrum of PLA contains three peaks at binding energy (BE) of 285.0, 287.0, and 289.1 eV, which was attributed to the C–C binding, ether and carboxyl groups respectively. The spectrum of Chol-Dex-CHO contains a major peak component at a binding energy of 286.3 eV, associated with the carbon bound with hydroxyl groups, and a minor component with BE at 287.8 ev, attributed to the ether groups on dextran skeleton. In addition, there are two small peaks appeared at 290 and 285 eV, which attributed to carboxyl from aldehyde groups and C–C binding from cholesterol components. The C_{1s} spectrum of nanoparticles was similar to that of pure Chol-Dex-CHO. The quantitative technique of XPS gives the average composition over a 5–7 nm depth inside the nanoparticle (Quellec et al., 1998), so the results

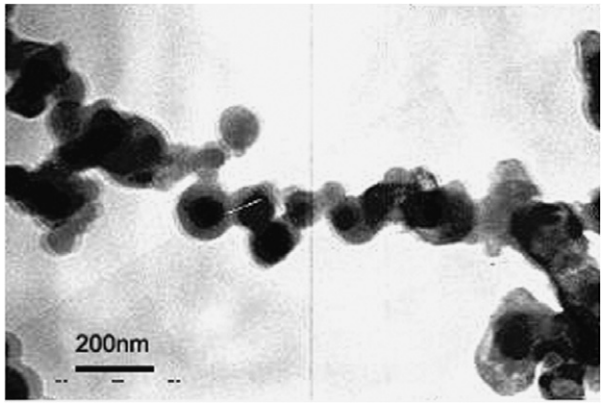

Fig. 6. Morphology of PLA/Chol-Dex-CHO nanoparticles observed by TEM.

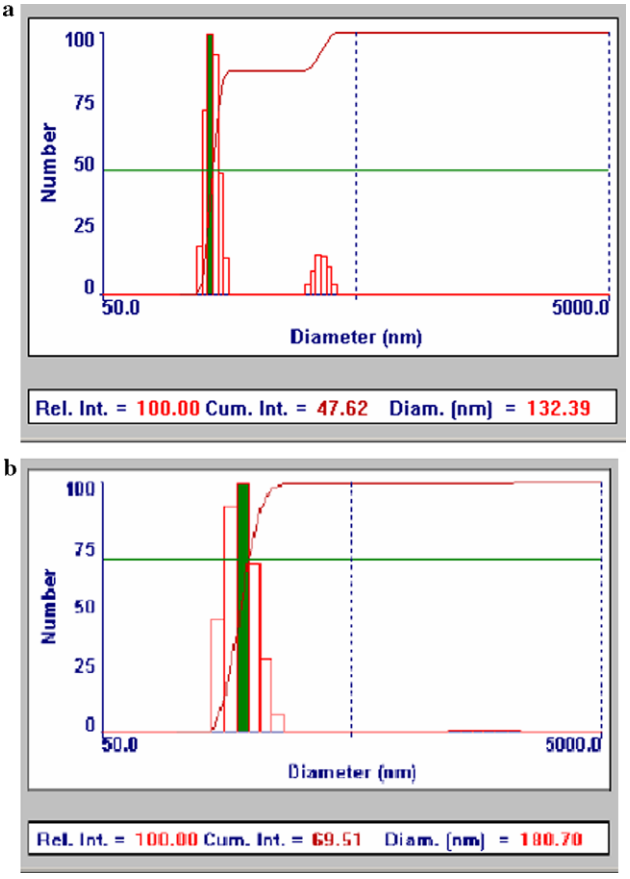

Fig. 7. Histograms of the size distribution of the PLA/Chol-Dex-CHO nanoparticles (a) and nanoparticles attached with transferrin (b).

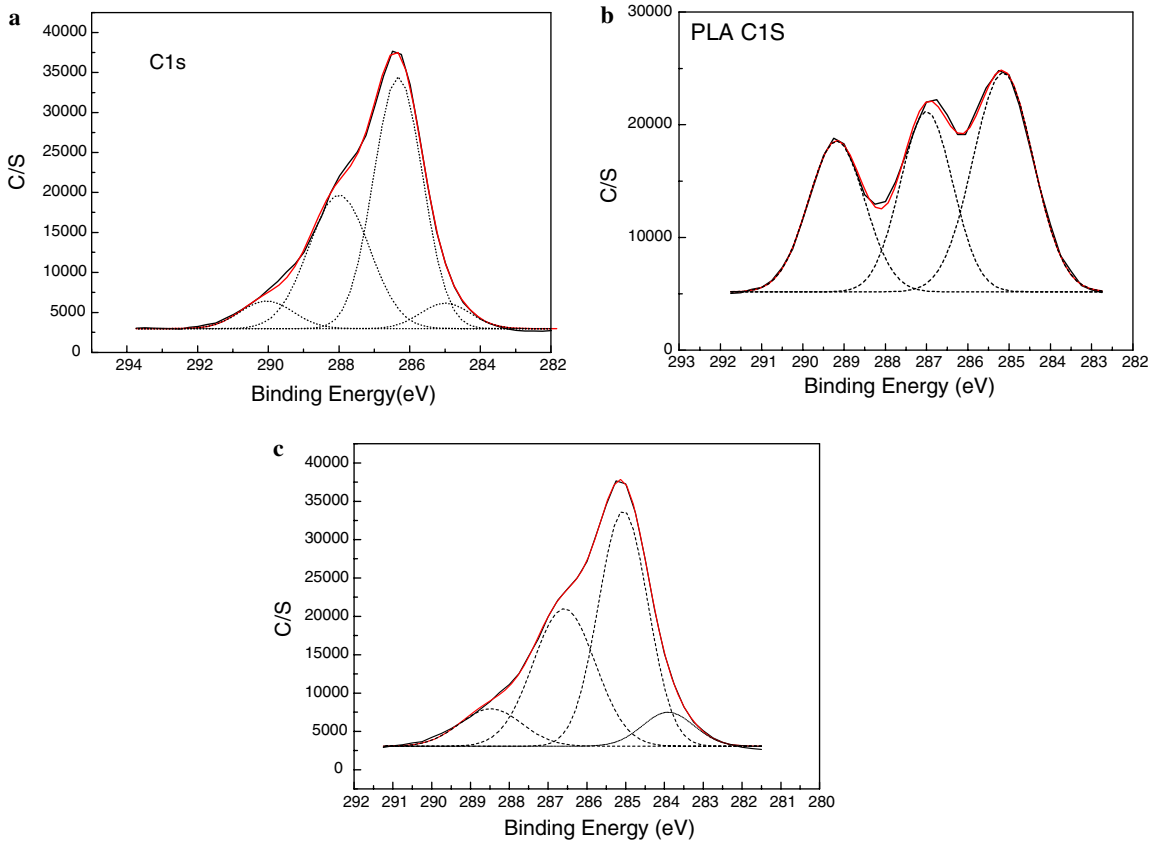

Fig. 8. XPS high-resolution C_{1s} spectra of (a) Chol-Dex-CHO, (b) Pure PLA, and (c) PLA/Chol-Dex-CHO nanoparticles.

of XPS suggest that the surface of nanoparticles obtained by co-dialysis method are coated with a thick layer of polysaccharide derivatives. This result is in accordance with the TEM image observation (Fig. 6), in which the core of nanoparticles was surrounded by a shell layer with a thickness of about 10 nm.

The result of XPS was confirmed by zeta potential analysis. The pure PLA particles exhibited a zeta potential value of −35.2 mV, while the self-aggregated PLA nanoparticles coated with Chol-Dex-CHO possess a zeta potential of −25.9 mV. This value was very close to that of Chol-Dex-CHO self-aggregated particles (−25.0 mV), demonstrating the presence of polysaccharide derivative on PLA nanoparticles.

3.4. Biofunctionalization of PLA/Chol-Dex-CHO nanoparticles

3.4.1. Determination of Chol-Dex-CHO conjugation and aldehyde content on surface of nanoparticles

The conjugation of Chol-Dex-CHO and the aldehyde content on surface of nanoparticles were quantitatively analyzed by Schales' method. When PLA/Chol-Dex-CHO nanoparticles were added to fuchsin solution, the pink color was occurred firstly on the surface of the PLA/Chol-Dex-CHO nanoparticles. This color development reaction further evidenced the existence of aldehyde groups. After developing for 30 min, a remarkable change in color of solution was observed. The amount of aldehyde groups on the nanoparticles was determined to be 0.052 mmol/mg nanoparticles, which means that 66.4% of Chol-Dex-CHO was conjugated on the surface of PLA nanoparticles.

3.4.2. Saturation for the TF coupled on nanoparticles

The saturation for the TF coupling on the nanoparticles was determined simply through plot the absorbance value (ABS value) of residual TF in supernatants versus weight ratio of TF to nanoparticles. As shown in Fig. 9, an inflexion appeared at the ratio of 0.03, and the ABS value was close to zero when ratio <0.03, while it increased with the amount of TF added when ratio >0.03. So the maximum amount for the TF coupling on the PLA/Chol-Dex-CHO nanoparticles calculated from this ratio is between 0.03 and 0.06 mg TF per milligram nanoparticles.

3.4.3. Evaluation of TF coupling on the PLA/Chol-Dex-CHO nanoparticles

The coupling of TF on PLA/Chol-Dex-CHO nanoparticles was evaluated by zeta measurement. After the attachment of transferrin, the zeta potential of the nanoparticles tended toward −2.8 mV, because of masking the negative charge of the core.

The coupling reaction was analyzed quantitatively by calculation of the difference between the initial TF amount and that remaining in the aqueous solution after nanoparticle

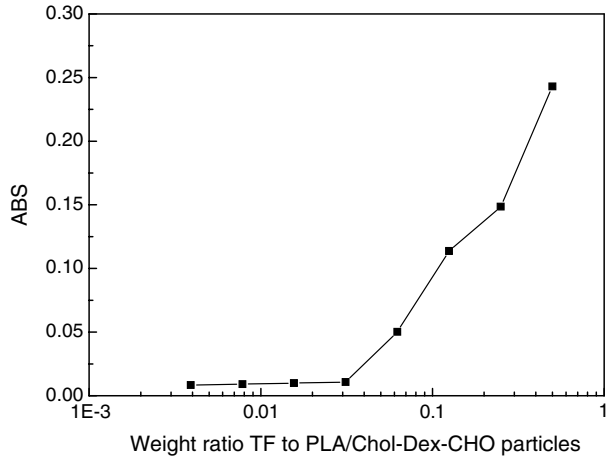

Fig. 9. Plot the absorbance value of residual TF in supernatants versus weight ratio of TF to nanoparticles.

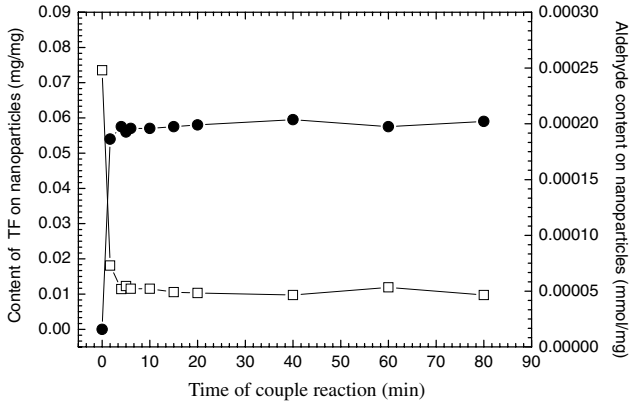

Fig. 10. Variety of TF and aldehyde amount on the surface of nanoparticles during the functionalization process. (●) Content of TF coupled on nanoparticles measured by UV-spectrophotometer (□) aldehyde groups content on the nanoparticles' surface measured by Schales' method.

removal. The amount of TF coupled on the nanoparticles as a function of reaction time is shown in Fig. 10. It is clear that the biofunctional reaction processed mainly in the first 5 min, and increasing reaction time had less significant effect on improving the reaction efficiency. To verify this result, residual aldehyde groups measurement was performed. Contrarily to that of TF, the aldehyde group on the nanoparticle surface decreased with reaction time, and a inflexion was occurred at 5 min point, corresponding to the TF curve.

The biofunctionalization reaction have a influence on size and size distribution of the PLA/Chol-Dex-CHO nanoparticles. As shown in Fig. 7b, the nanoparticle size increased by about 50–70 nm after coupling of TF, and the size distribution is broad slightly. No apparent change in morphology, however, was observed by TEM.

3.4.4. Influence of biofunctionalization on drug leakage and release

As mentioned before, inappropriate coupling method might lead to the leakage of the entrapped drug, resulting in the fail in clinic application. One of the main purpose of this paper was to study the relationship between the leakage of the drug preloaded in the nanoparticles and the process of covalent coupling. Except for biotin–avidin physical conjugation, typical ligand coupling method is acylation in the presence of carbodiimide, the reaction is generally performed over 2 h (Stella et al., 2000). We measured the amount of IMC leaked to the reaction medium at defined time of biofunctionalization. The result (Fig. 11) indicated that the leakage ratio was only 5.6% after 5 min, and reached 31.5% when the reaction was finished after 80 min. It was obvious that the drug loaded in nanoparticle leaked rapidly along with the reaction processed.

Due to the instability of Schiff's base linkage, the ligand-coupled nanoparticles should be further treated with $NaBH_4$ for 10 min. After all of the procedures described above, only 16.2% IMC preloaded in nanoparticles leaked. So if there is no negative-effect on bioactivity of ligand, the Schiff's base reaction should be a feasible way for quick coupling of ligand to drug-loaded nanoparticles.

The release profiles of IMC from TF-bound and non-bound nanoparticles in phosphate buffer solution (pH 7.4) at 37 °C are shown in Fig. 12. Both of them exhibited tri-phasic release behavior, that is an initial burst of about 35% for 14 h, a second phase for up to 90 h, followed by a third phase sustain release of drug thereafter. However, TF-bound nanoparticle and non-bound ones displayed different release profiles. The non-bound ones (curve a) were released about 50% in 1 week through a big initial burst and almost linear release then. A similar release profile was obtained by TF-bound sample (curve b), excepting with a smaller initial burst. It has been suggested that the initial burst release arose from the dissolution of drug close to or at the surface of carrier (Peracchia et al., 1997; Ubrich, Bouillot, Pellerin, Hoffman, & Maincent, 2004; Matsumoto, Nakada, Sakurai, Nakamura, & Takahashi, 1999). The pro-treatment of nanoparticles in solution during functionalization process eliminated the drug that associated on the nanoparticle surface, leading to the

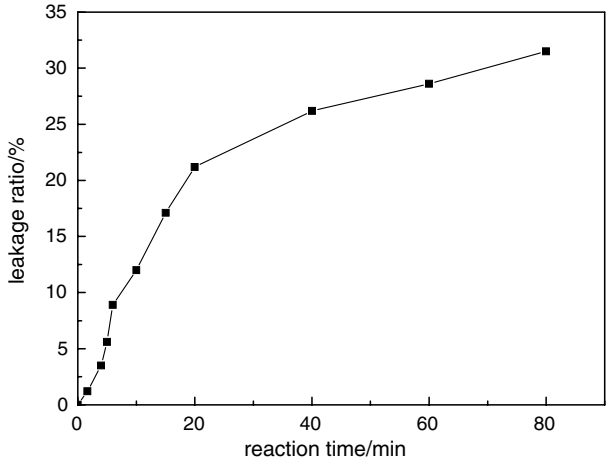

Fig. 11. Plot of drug leakage ratio versus the biofunctionalization reaction time.

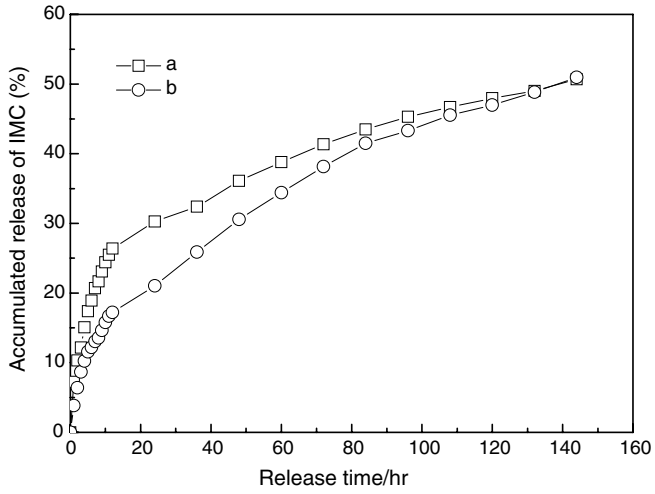

Fig. 12. Release profile of IMC from TF-bound (○) and non-bound (□) PLA/Chol-Dex-CHO nanoparticles.

weakening in initial burst release. Considering that sample a and b displayed nearly the same release pattern, it can be concluded that there was no obvious influence of TF-bound biofunction in the in vitro release test.

3.4.5. Tumor cell uptake of TF-bound PLA nanoparticles

Internalization of TF-bound PLA nanoparticles by U251 glioma cells was employed to confirm the activity of the TF on the nanoparticles surface and the target ability of nanoparticles. After incubating tumor cells with nanoparticles at 37 °C, TF-bound PLA nanoparticles, detected by fluorescent phase-contrast microscopy, gathered at margin of glioma cells at 2 h and internalized by tumor cells within 4 h (Fig. 13a). To make a control, adipic dihydrazide modified Chol-Dex-CHO (Chol-Dex-NH_2) was synthesized by condensation of hydrazide with aldehyde groups, therefore amino groups was introduced into Chol-Dex molecules to facilitate the FITC labeling. Chol-Dex-NH_2 coated PLA nanoparticles (PLA/Chol-Dex-NH_2) was prepared and fluorescence labeled using same procedure as that of PLA/Chol-Dex-CHO, and no gather around of glioma cells by these nanoparticles were found at same time intervals and the cell uptake was remarkably slow (Fig. 13b).

4. Conclusion

Cholesterol hydrophobic modified dextran dialdehyde was successfully synthesized. Its amphiphilic characteristic was confirmed by surface tension and fluorescence spectrum measurement. It was used as stabilizers to produce polysaccharide coated PLA nanoparticles by co-dialysis method with a mean diameter of 100–150 nm. TEM observation, zeta measurement and XPS analysis proved that the polysaccharide derivatives were securely anchored on the nanoparticles surface, and fuchsin-spectrophotometer measurement demonstrated the existence of aldehyde groups. Transferrin was coupled to nanoparticles surface by taking advantage of the Schiff's base reaction. The coupling process reached equilibrium within 5 min and less than 20% drug was leaked after $NaBH_4$ reduction. TF coupled nanoparticles can bind target to glioma tumor cell. This study

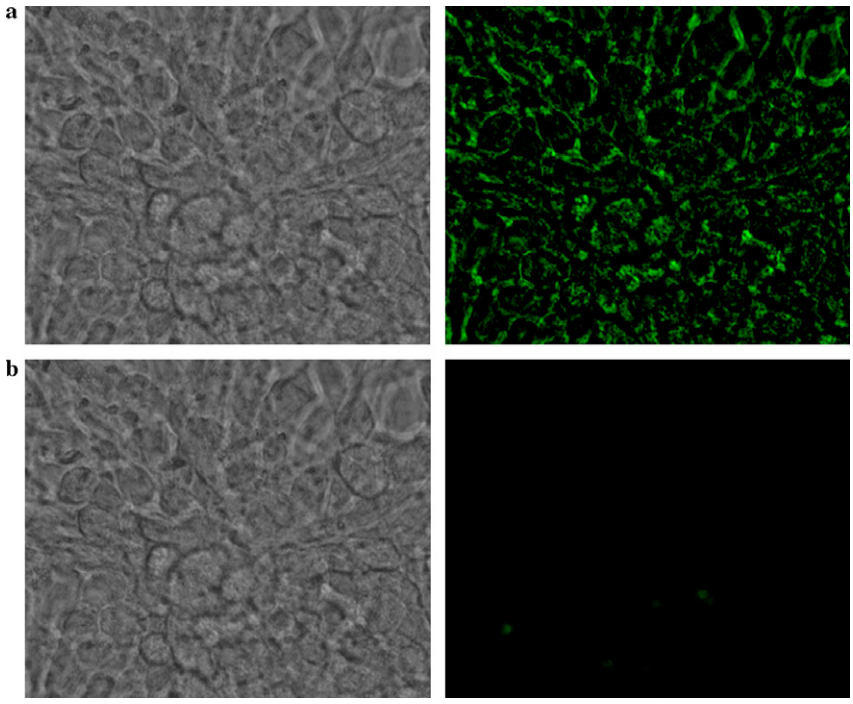

Fig. 13. Phase-contrast images of U251 glioma cells (left) and fluorescent micrographs of internalization of PLA nanoparticles (right). (a) TF-bound PLA nanoparticles and (b) Chol-Dex-NH_2 coated PLA nanoparticles, within 4 h.

showed that Chol-Dex-CHO surface decoration of nanoparticles was a potential way for the bioactivity conjugation and drug delivery target to tumor.

Acknowledgment

This paper was financially supported by the National Natural Science Foundation of China (Grant No. 50573056).

References

Alami, E., Almgren, M., Brown, W., & Francois, J. (1996). Aggregation of hydrophobically end-capped poly(ethylene oxide) in aqueous solutions: fluorescence and light-scattering studies. *Macromolecules, 29*(6), 2229–2243.

Allen, T. M. (1994). The use of glycolipids and hydrophilic polymers in avoiding rapid uptake of liposomes by the mononuclear phagocyte system. *Advanced Drug Delivery Reviews, 13*(3), 285–309.

Bazile, D., Prud-Homme, C., Bassoullet, M. T., Malard, M., Spenlehauer, G., & Veillard, M. (1995). Stealth MePEG-PLA nanoparticles avoid uptake by the mononuclear phagocytes system. *Journal of Pharmaceutical Sciences, 84*, 493–498.

Choi, S. W., Kim, W. S., & Kim, J. H. (2003). Surface modification of functional nanoparticles for controlled drug delivery. *Journal of Dispersion Science and Technology, 24*(3–4), 475–487.

Dumitriu, S. (2001). Polysaccharides as biomaterials. In S. Dumitriu (Ed.), *Polymeric biomaterials* (pp. 1–61). New York: Marcel Dekker.

Imoto, T., & Yanagishita, K. (1971). A simple measurement of lysozyme. *Agricultural and Biological Chemistry, 35*(7), 1154–1156.

Kuhn, R. W., Schrader, W. T., Smith, R. G., & O'Malley, B. W. (1975). Progesterone binding components of chick oviduct X. Purification by affinity chromatography. *The Journal of Biological Chemistry, 250*(11), 4220–4228.

Lee, K. Y., Jo, W. H., Kwon, I. C., Kim, Y. H., & Jeong, S. Y. (1998). Physicochemical characteristics of self-aggregates of hydrophobically modified chitosans. *Langmuir, 14*(9), 2329–2332.

Lemarchand, C., Gref, R., & Couvreur, P. (2004). Polysaccharide-decorated nanoparticles. *European Journal of Pharmaceutics and Biopharmaceutics, 58*(2), 327–341.

Lundberg, B. B., Griffiths, G., & Hansen, H. J. (2000). Specific binding of sterically stabilized anti-B-cell immunoliposomes and cytotoxicity of entrapped doxorubicin. *International Journal of Pharmaceutics, 205*(1–2), 101–108.

Magmy, B., Iliopoulos, I., Zana, R., & Audebert, R. (1994). Mixed micelles formed by cationic surfactants and anionic hydrophobically modified polyelectrolytes. *Langmuir, 10*(9), 3180–3187.

Maiti, S., Jayachandran, K. N., & Chatterji, P. R. (2001). Probing the association behavior of poly(ethyleneglycol) based amphiphilic comb-like polymer. *Polymer, 42*(18), 7801–7808.

Matsumoto, J., Nakada, Y., Sakurai, K., Nakamura, T., & Takahashi, Y. (1999). Preparation of nanonanoparticles consisted of poly(L-lactide)-poly-(ethyleneglycol)-poly(L-lactide) and their evaluation in vitro. *International Journal of Pharmaceutics, 185*(1), 93–101.

Mora, P. C., & Baraldi, P. G. (2002). Democosmetic applications of polymeric biomaterials. In S. Dumitriu (Ed.), *Polymeric biomaterials* (pp. 459). New York: Marcel Dekker.

Nichifor, M., Lopes, A., Carpov, A., & Melo, E. (1999). Aggregation in water of dextran hydrophobically modified with bile acids. *Macromolecules, 32*(21), 7078–7085.

Nobs, L., Buchegger, F., Gurny, R., & Allemann, E. (2004). Current methods for attaching targeting ligands to liposomes and nanoparticles. *Journal of Pharmaceutical Sciences, 93*(8), 1980–1992.

Peracchia, M. T., Gref, R., Minamitake, Y., Domb, A., Lotan, N., & Langer, R. (1997). PEG-coated nanospheres from amphiphilic diblock and multiblock copolymers: investigation of their drug encapsulation and release characteristics. *Journal of Controlled Release, 46*, 223–231.

Quellec, P., Gref, R., Perrin, L., Dellacherie, E., Sommer, F., Verbavatz, J. M., et al. (1998). Protein encapsulation within polyethylene glycol-coated nanospheres. I. Physicochemical characterization. *Journal of Biomedical Materials Research, 42*, 45–54.

Rouzes, C., Gref, R., Leonard, M., & Dellacherie, E. (2000). Surface modification of poly(lactic acid) nanospheres using hydrophobically modified dextrans as stabilizers in an o/w emulsion/evaporation technique. *Journal of Biomedical Materials Research, 4*(50), 557–565.

Rouzes, C., Durand, A., Leonard, M., & Dellacherie, E. (2002). Surface activity and emulsification properties of hydrophobically modified dextrans. *Journal of Colloid and Interface Science, 253*(1), 217–223.

Schacht, E., Bogdanov, B., Van Der Bulcke, A., & De Rooze, N. (1997). Hydrogels prepared by crosslinking of gelatin with dextran dialdehyde. *Reactive & Functional Polymers, 33*(2), 109–116.

Stella, B., Arpicco, S., Peracchia, M. T., Desmaele, D., Hoebeke, J., Renoir, M., et al. (2000). Design of folic acid conjugated nanoparticles for drug targeting. *Journal of Pharmaceutical Sciences, 89*(11), 1452–1464.

Stenekes, R. J. H., Talsma, H., & Hennink, W. E. (2001). Formation of dextran hydrogels by crystallization. *Biomaterials, 22*(13), 1891–1898.

Svetlana, N. D., Ludmila, S. I., Alexander, R. K., & Elena, V. E. (1996). Aldo-enol transition in periodate-oxidized dextrans. *Carbohydrate Research, 280*(1), 171–176.

Ubrich, N., Bouillot, P., Pellerin, C., Hoffman, M., & Maincent, P. (2004). Preparation and characterization of propranolol hydrochloride nano-nanoparticles: a comparative study. *Journal of Controlled Release, 97*, 291–300.

Vieira, N. A. B., Moscardini, M. S., & Tiera, M. J. (2003). Aggregation behavior of hydrophobically modified dextran in aqueous solution: a fluorescence probe study. *Carbohydrate Polymers, 53*(2), 137–143.

Woodle, M. C., & Lasic, D. D. (1992). Sterically stabilized liposomes. *Biochimica et Biophysica Acta, 1113*(2), 171–199.

Zipser, B., Bradford, J. J., & Hollingsworth, R. I. (1998). Cholesterol and its derivatives, are the principal steroids isolated from the leech species *Hirudo medicinalis*. *Comparative Biochemistry and Physiology Part C, 120*(2), 269–282.